An analysis of flow induced formation of long fibers

Janssen, L.P.B.M.; Janssen-van Rosmalen, R.

Published in:
Rheologica Acta

DOI:
10.1007/BF01522030

Publication date:
1978

Rheol. Acta **17**, 578 – 588 (1978)

ISSN 0035-4511 / ASTM-Coden: RHEAAK

Department of Chemical Engineering, University of Delaware, Newark, Del. (USA)

An analysis of flow induced formation of long fibers

*L. P. B. M. Janssen**), and *R. Janssen-van Rosmalen***)

With 6 figures

(Received February 6, 1978)

Nomenclature

b	surface layer thickness
C	constant
c	concentration
$\boldsymbol{d}$	rate of strain tensor
F	free energy
F_K	kink energy
F_V	free energy far from the fiber
G	growth rate constant
H	enthalpy
K	ratio between tube diameter and fiber diameter
L	filament length
l	length of the critical nucleus
Q	flow rate
R	fiber diameter
R^*	gas constant
r	radial coordinate
S	entropy
S^f	internal entropy in the fluid phase
S^s	internal entropy in the solid phase
T	temperature
$T_{m,d}$	melting or dissolution temperature
T_d	dissolution temperature
t	time
u	axial fluid velocity
V	difference between draw velocity and maximal fluid velocity
V_D	draw velocity
V_F	maximal fluid velocity without fiber
V_G	fiber grow velocity
$\boldsymbol{v}$	velocity vector
Z_u	length of the "entrance length" upstream of the fiber tip
z	axial coordinate
α	constant, depending on the nucleation model
Γ	total stretch
γ	activity coefficient
$\dot{\Gamma}$	shear rate or stretch rate
δ	boundary layer thickness
ζ	characteristic length
η	viscosity
η_{el}	elongational viscosity
η_{sh}	shear viscosity
θ	relative temperature difference
Λ	time constant
μ	driving force
ρ	density
σ'	tensile strength of the fiber
σ	lateral surface free energy
σ_e	fold surface free energy
τ	excess stress tensor co-ordinated to the polymer molecules
χ	lattice restriction constant

1. Introduction

Phenomena of strain-induced crystallization, and more specifically of flow-induced fiber formation, have been well documented in the literature (1 – 7). Fibers with very good mechanical properties have been grown from flowing polymer solutions (8 – 10) under conditions of temperature and concentration such that, in the absence of flow, the driving force for crystallization would be small or even negative, i.e., fibers could in fact have a tendency to dissolve rather than to grow.

A recent paper by *McHugh* et al. (10) reports experimental observations on fiber growth from a seed in a Poiseuille flow. They observed that a fast "primary" growth in axial and radial direction results in rapid formation of a filament with a constant diameter of the order of 40 μm; this is followed by a slow "secondary" growth in the radial direction which starts at the seed and results in final fiber diameters of the order of 400 μm.

In this paper we suggest a semi-quantitative analysis of the primary fiber growth phenomenon as observed experimentally. We adopt an engineering viewpoint in the analysis; we wish to introduce methods by which the whole phenomenon could be modeled to the point of obtaining quantitative predictive ability, even

*) On leave from the Laboratory for Physical Technology Delft University of Technology, Delft (The Netherlands).

**) On leave from the RIM Laboratory for Solid State Physics, Catholic University Nijmegen (The Netherlands).

if at the cost of adopting order-of-magnitude estimates of the significant parameters and variables. The dependency of the final fiber diameter on the local shear and temperature is clearly shown in practice (8, 10). The prediction of the influence of rheology, capillary diameter and throughput on the growth process as indicated by this analysis, still needs experimental verification.

The phenomena considered are remarkably complex, and we focus attention on three main issues; the fluid mechanics involved, the molecular structure of the fluid from which the fiber is grown, and the crystal growth phenomenon itself.

2. Driving force for fiber formation

It is generally recognized that flow-induced fiber growth is related to the tendency of polymer molecules to elongate and align in a flow field. Such elongation and alignment result in a decrease of conformational entropy, so that the partial molar free energy of a polymer in a flowing solution or melt may be appreciably higher than it is in the absence of flow. Therefore, in a flowing solution or melt, there may be a positive driving force for crystallization even if in the absence of flow the driving force would be negative.

A more quantitative formulation of the argument given above is as follows. The driving force for crystallization is determined by the difference between the chemical potential of the polymer in the fluid and the crystal phases:

$$\Delta\mu = \Delta H - T\Delta S \qquad [1]$$

where H is the enthalpy and T the absolute temperature. The entropy difference ΔS can be estimated as follows (11 – 12):

$$\Delta S = \chi + S^f - S^s - R^* \ln \gamma c \qquad [2]$$

where S^f and S^s are the internal entropies of the polymer molecules in the fluid and solid phases, χ is the communal entropy and accounts for the absence of lattice restrictions for the fluid-phase polymer, R^* is the gas constant, γ is the activity coefficient and c is the fraction of the solution cells which is occupied by solute molecules, and can be expressed by an appropriate concentration measure in the fluid phase.

One may safely assume that, for small displacements from equilibrium because of flow field and concentration, ΔH has the same value as at equilibrium, say:

$$\Delta H = (T\Delta S)_{eq}. \qquad [3]$$

This assumption embodies the idea that, while flow may induce changes of conformational entropy, it does not induce variations of internal energy. Indeed, the assumption that whatever elasticity a polymeric fluid may have is entirely entropic has been studied theoretically in detail (13), and has been shown experimentally to be acceptable (14).

Since in equilibrium $\Delta\mu_{eq} = 0$, we are allowed to subtract this from eq. [1]. Combination of eqs. [1] and [2], and taking eq. [3] into account, gives:

$$\Delta\mu = \{T[\chi_{eq} - \chi] - T[S^f - S^f_{eq}]\} + R^* T \ln \frac{\gamma c}{(\gamma c)_{eq}}. \qquad [4]$$

In the absence of flow, and under the assumption that the influence of entanglements does not change much for small displacements from equilibrium, the term in curled brackets on the right hand side of eq. [4] can be approximated by zero, so that:

$$\Delta\mu = R^* T \ln \frac{\gamma c}{(\gamma c)_{eq}} \qquad [5]$$

which, under the additional assumptions that $\gamma_{eq} \approx \gamma$, and that $\Delta\mu$ is small, can be linearized to:

$$\Delta\mu = R^* T \frac{c - c_{eq}}{c_{eq}}. \qquad [6]$$

Eq. [6] is the classical no-flow result that the driving force for crystallization is proportional to the supersaturation.

In the presence of a flow field, the term in curled brackets on the right hand side of eq. [4] is not zero; if ΔS_{flow} is the flow-induced decrease of conformational entropy, and under the same assumptions leading from eq. [5] to eq. [6], one obtains:

$$\Delta\mu = T\Delta S_{flow} + R^* T \frac{c - c_{eq}}{c_{eq}}. \qquad [7]$$

Eq. [7] shows that $\Delta\mu$ may be positive even when c is less than c_{eq}.

Although the expressions for the driving force (eqs. [6] and [7]) are quite simple under certain restrictions, a solubility curve is necessary for

both cases. However, it is very difficult to determine the equilibrium concentration, which may be the reason that there are no such curves given in the literature.

Therefore it is feasible to use a simpler expression for the driving force. This can be obtained directly from eq. [1] in combination with eq. [3] under the assumption that ΔH may be taken constant within the small temperature differences as applied in fiber growth processes:

$$\Delta\mu = T\Delta S_{\text{flow}} + \frac{T_{m,d} - T}{T_{m,d}}\Delta H \qquad [8]$$

where $T_{m,d}$ is the melting temperature in the case of melt or the dissolution temperature in the case of solutions. Again, eq. [8] shows that $\Delta\mu$ may be positive even if the temperature of the melt or solution is higher than the melting or dissolution temperature.

We will now consider the growth process in more detail by introducing a scheme for the energy barriers a molecule must overcome to enter an energetically favored place on the surface (15, 16). We will consider a situation that the solution or melt is stirred (fig. 1), and that the fiber would dissolve without a flow field. The free energy content F of a molecule as a function of its place is given. Several subprocesses can be distinguished. Molecules diffuse from the bulk to the crystal surface as a result of a free energy gradient; they have to deal with the activation free energy $\Delta F_{v\,\text{diff}}$, that determines the diffusion jump from one equilibrium position in the solution to a neighboring one. Far from the fiber the stretching of molecules as a result of a shear field is generally not very effective, so that in that case the free energy F_v is about the same as that without a flow field. Near the surface the free energy content goes up by an amount $|T\Delta S|_{\text{flow}}$. In the interface the molecules must be separated from the solvent, and a certain disentanglement takes place: so ΔF_{ads} determines the entering of the surface adsorption layer. ΔF_{deads} determines the leaving of the same layer. ΔF_{surf} must be taken into account when the molecules are physically absorbed on the surface prior to crystallization (17). Finally, the growth unit must overcome an energy ΔF_k (this value depends on the lengths of the chain folds) to enter an energetically favored place (kink) on the surface.

The difference in chemical potential

$$\Delta\mu = F_v + |T\Delta S|_{\text{flow}} - F_k \qquad [9]$$

determines the driving force for crystallization. This energy scheme gives only a rough survey of the main processes occurring during growth, and does not include any description of the process of chain folding.

3. Fluid mechanics

In order to express eqs. [7] and [8] in a more quantitative way, an estimate of ΔS_{flow} is needed. Obtaining such an estimate requires an appropriate modeling of the molecular structure of the polymeric fluid; of course, this molecular

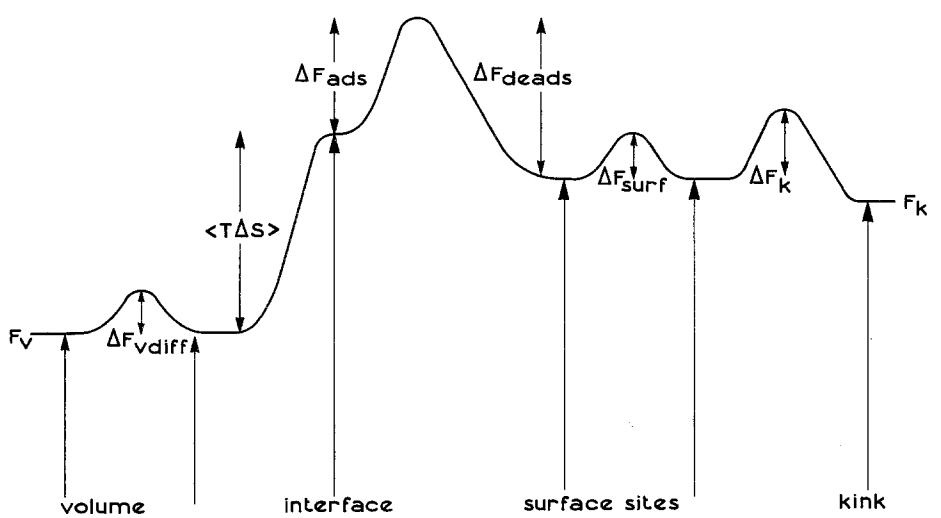

Fig. 1. Energy barriers that a molecule must overcome to enter an energetically favored place on the surface

model must include the influence of flow kinematics.

Although many molecular models for polymeric fluids have been developed, they are generally purely mechanical models, i.e., they allow calculation of the stresses induced by flow but not of the entropy changes. More recently the thermodynamic analysis of some of these models has been carried out (18); a general analysis of the connection between such molecular model and the continuum thermodynamic theory of polymers is available (19); a recent paper reviews the state of the art of the modeling of flow-induced changes of conformational entropy (20). The mathematical complexity of these more general analyses is rather impressive, and for the purpose of the engineering analysis to be developed here, we refer specifically to the thermodynamic model of a suspension of linear elastic dumbbells developed by *Marrucci* (20). For *Marrucci*'s model, the entropy change due to flow is given by:

$$\Delta S_{\text{flow}} = \frac{\text{tr}\,\boldsymbol{\tau}}{2cT} \qquad [10]$$

where tr τ is the trace of the excess stress tensor co-ordinated to the polymer molecules.

Even after a molecular model has been selected, an analysis of the fiber growth phenomenon requires explicit consideration of the fluid mechanics involved. This in turn implies the choice of a constitutive equation, the logical one being, of course, the one that is produced by the molecular model chosen; in the case of *Marrucci*'s model, this would dictate adoption of the contravariant Maxwell model:

$$\boldsymbol{\tau} + \Lambda \frac{\mathscr{D}\boldsymbol{\tau}}{\mathscr{D}t} = \eta \boldsymbol{d} \qquad [11]$$

where Λ is the time constant, η the viscosity, $\boldsymbol{d}$ the rate of strain tensor and $\mathscr{D}\boldsymbol{\tau}/\mathscr{D}t$ the Oldroyd contravariant convected derivative given by

$$\frac{\mathscr{D}\boldsymbol{\tau}}{\mathscr{D}t} = \frac{\partial \boldsymbol{\tau}}{\partial t} + \boldsymbol{v} \cdot \nabla \boldsymbol{\tau} - \boldsymbol{\tau} \cdot \nabla \boldsymbol{v} - (\nabla \boldsymbol{v})^T \cdot \boldsymbol{\tau} \; . \qquad [12]$$

The equations of motion for the contravariant Maxwell model can easily be solved far upstream and far downstream of the fiber tip, where the flow field is essentially the same as for a Newtonian solution. It is, however, presumably out of the question to obtain an analytical solution for the flow near the fiber tip, not only because of the mathematical complexity involved but also because of the rather sketchy knowledge of the actual shape of this tip, which makes it difficult to establish the appropriate boundary conditions.

4. Flow field around the fiber

The most complete analysis of the fluid mechanics involved in fiber growth is given by *Mackley* (22). He considered creeping flow around an elongated ellipsoid at zero incidence, and could apply this model to the growth of small fibers in the entrance region of a jet, for growth from solution (23) as well as from the melt (26). The elongational velocity gradients near the tip appeared to be much larger than the shear rate in *Mackley*'s model.

An extension of this model to the growth of very long fibers as they are grown by placing a seed in the solution (8 – 10) would involve the following problems:

(i) The filament resulting from the primary growth has essentially a constant diameter (10), so that an ellipsoid does not seem to be a good geometrical analogy. A better description of the morphology would be given by a rod, but it is well-known that there is no non-trivial steady-state solution for the equations of motion for creeping flow parallel to an infinite long rod in an infinite fluid.

(ii) Flow around an ellipsoid is strongly influenced by the leading edge kinematics, while a fiber grown from a fixed seed or one continuously withdrawn from the fluid has no leading edge.

(iii) This model does not include the influence of the vessel dimensions on the fiber growth. Since no steady state solution for an infinite long rod in an infinite liquid exists, it is obvious that for the growth of long fibers after a certain entrance region the vessel geometry plays an important role in the fluid dynamics.

We therefore choose to analyse the following geometrical configuration:

Consider a cylindrical filament at the axis of the tube. The problem reduces to axial laminar flow in an annulus region between two concentric cylinders in the part of the tube where the fiber is present and to a simple Poiseuille flow where there is no fiber in the tube (fig. 2). The inner cylinder (fiber) is moving with a velocity equal to the draw velocity V_D and there

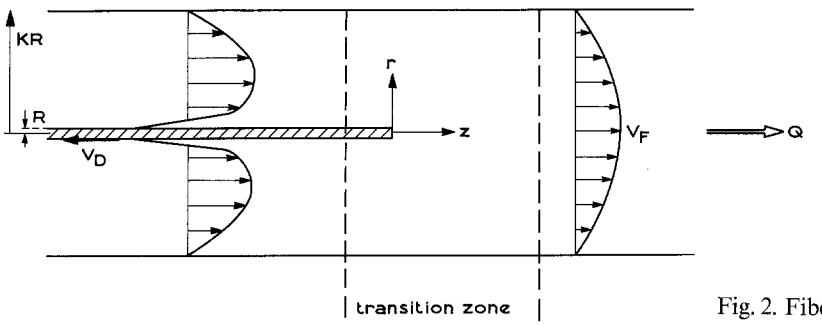

Fig. 2. Fiber growth in a Poiseuille flow

is a net throughput $-Q$ through the system. Taking r, z, and θ as the 1, 2, and 3 direction respectively, it is easy to show that sufficiently far from the fiber tip the stress deviator for a contravariant Maxwell model equals

$$\tau = \eta \begin{pmatrix} 0 & \dot{\Gamma} & 0 \\ \dot{\Gamma} & 2\Lambda\dot{\Gamma}^2 & 0 \\ 0 & 0 & 0 \end{pmatrix} \qquad [13]$$

which justifies a Newtonian solution for the flow field. When the pipe to fiber diameter ratio K is much larger than unity (as is obviously always the case), the following result is obtained for the shear rate at the filament surface

$$\left.\frac{du}{dr}\right|_{r=R} = \left(\frac{V_D}{R} - \frac{2Q}{\pi K^2 R^3}\right)\left(\frac{1}{1 - \ln K}\right). \qquad [14]$$

When we introduce V_F as the fluid velocity which would prevail at the tube axis if there were no fiber present and V the difference between the draw velocity and V_F, eq. [14] reduces to

$$\left.\frac{du}{dr}\right|_{r=R} = \frac{V}{R}\frac{1}{1 - \ln K}. \qquad [15]$$

Contrary to *Mackley*'s result (22) eq. [15] takes also the pipe diameter into account. The velocity gradient at the fiber wall goes to zero when the pipe diameter goes to infinity (although very slowly).

The interesting problem now is how far downstream from the filament tip is this well-developed velocity profile indeed reached. In order to make such an estimation one could attack the cylindrical boundary layer problem for an annulus directly which in fact leads to a closed form solution in the case of a Newtonian fluid.

One does not, however, need to use explicitly such a closed form solution, since a simple order-of-magnitude analysis of the classical boundary layer type leads immediately to:

$$\left.\frac{du}{dr}\right|_{r=R} = \sqrt{\frac{V^3\rho}{|z|\eta}} \qquad [16]$$

where ρ and η are the density and viscosity of the fluid, and $|z|$ is the distance from the tip. Since the flow field is essentially a shear flow, it seems appropriate to take η as the shear viscosity of the fluid. As expected, the shear rate at the fiber surface decreases with increasing $|z|$, and an estimate of the length Z_u required for development of the velocity profile is obtained by requiring the right hand side of eqs. [15] and [16] to coincide; this yields:

$$\frac{Z_u}{R} = \mathrm{Re}\,(1 - \ln K)^2 \qquad [17]$$

where Re is the Reynolds number based on the fiber radius and the relative velocity V.

Even if very dilute solutions with viscosities of only a few centipoises are considered, the value of Re for a 40 μm filament is at most of order unity; in concentrated solutions or melts that value would be of the order of 10^{-2} or even much less than that. Values of K are no more than 10^4, so that the right hand side of eq. [17] would at most be of order 10, and very likely much less than that. The upstream velocity profile develops within at most a few filament radii, so that to all practical purposes the entire filament may be considered as exposed to the velocity profile prevailing at $z \to -\infty$, i.e., to a shear rate given by eq. [15].

The flow field downstream of the fiber tip is mainly an elongational flow. Although in our case an exact analytical treatment of this elongational flow cannot be given an estimation of the stretch near the fiber can be made. We therefore choose first to analyse the elongation downstream from a non-growing fiber and we

anchore the coordinate system to the fiber tip, located at $z = 0$. Far downstream of the fiber an undisturbed Poiseuille flow can be assumed and its center velocity with respect to the tip equals $V_F + V_D = V$ (fig. 3). For an order of magnitude estimation we generalize *Mackley*'s

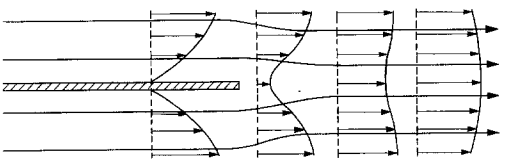

Fig. 3. Qualitative streamline pattern around a non-growing seed

solution for the elongational flow downstream of an ellipsoid to

$$u = V\left(1 - \frac{\ln(\zeta/z)}{C}\right) \qquad [18]$$

where ζ is some characteristic axial length much larger than the distance z over which we look and C is a geometrical parameter. In fact the magnitude of these parameters is related to the shear stresses at the fiber wall, and in *Mackley*'s analysis they are given by the magnitude of the ellipsoid axes. For our order of magnitude estimation we may leave them undefined.

Differentiating eq. [18] with respect to z gives the stretch rate downstream of the fiber tip:

$$\dot{\Gamma}_{zz} = \frac{\partial u}{\partial z} = \frac{V}{Cz}. \qquad [19]$$

However, it should be pointed out that the flow downstream of the fiber tip is from a Lagrangian point of view an unsteady elongation. The material is only elongated for a finite length of time. Therefore it is not the stretch rate but the total stretch that is important for the growth process (25); if we assume for this order-of-magnitude estimation the molecular stretch to be of the order of the fluid stretch we have to integrate eq. [19] with respect to time:

$$\Gamma_{zz} = \int \frac{\partial u}{\partial z}\, dt = \int \frac{\partial u}{\partial z}\frac{1}{u}\, dz. \qquad [20]$$

After substitution of eqs. [18] and [19] in this equation we obtain

$$\Gamma_{zz} = \int \frac{dz}{z(C - \ln(\zeta/z))} \qquad [21]$$

which can easily be integrated to give:

$$\Gamma_{zz} = \ln\left[\ln\left(\frac{\zeta}{z}\right) - C\right] + \text{constant}. \qquad [22]$$

Without going into further details concerning the various constants it is clearly evident that the total stretch of the molecules very close to the fiber tip is very large.

Another solution for a wake downstream an axial symmetric body is given by *Schlichting* (26). Although this solution is inaccurate at short distances from the fiber tip its limiting behavior is also a logarithm of the reciprocal distance.

It has to be realized that all these solutions are for a non-growing body, where all side walls are stationary with respect to the tip. In fact this solution could be compared with the flow around the seed before the fiber actually starts growing. As shown in figure 3 the elongation is downstream of the tip and not very effective since a molecule that has once passed the tip generally would not reach this tip anymore but is carried away, no matter how much the stretch is. Only molecules that are attached to the seed just before they would leave the tip can contribute to the initiation of the axial growth.

Once the fiber starts growing and a critical growth velocity has been exceeded the situation changes quite dramatically. This can most easily be seen when the fiber is drawn at the same velocity as it grows, which means that the growing tip remains stationary but the fiber wall has a velocity $-V_D$. This introduces an extra backflow as is shown in the qualitative stream line pattern of figure 4. The elongated molecules now can reach the tip very easily and it also gives rise to renewal of solution near the tip, thus mitigating the diffusion of polymeric material from the bulk of the fluid to the tip as a limiting factor in the growth.

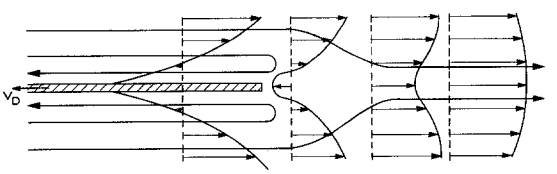

Fig. 4. Qualitative streamline pattern around the growing fiber

It is by no means sure that the total stretch remains unchanged in comparison with the no-growth analysis. However since there is a certain similarity between the development of

the velocity profiles in the two cases it is still to be expected that the total stretch near the fiber tip is extremely large.

A similar argument can be used when the fiber is stationary while the tip is growing, as for instance is the case in *McHugh*'s experiments (10). In this case we can attach the coordinate system to the growing tip which implies at once that the fiber walls have a velocity $-V_D$ with respect to the tip itself. As long as the growth velocity is smaller than the maximal velocity which prevails in an empty tube this would imply that the argumentation is qualitatively the same as for the drawn fiber. Since the elongation is very high it seems from hydrodynamical point of view that the only restriction to the axial flow ir that it cannot be larger than the local fluid velocity.

The predictions of this qualitative model can also explain the initiation of the growth process (27). Once the seed is placed in the flowing solution it takes a certain time before the fiber starts growing. This initiation time is quite unpredictable and varies roughly between 5 seconds and 5 minutes, independent of whether an artificial or a natural seed has been used. This can be related to the difficulties of the elongated molecules to attach to the non-growing seed as described before. After this initiation time, once the fiber starts growing it grows very rapidly indeed.

It has to be realized that other constraints can be put on the primary axial growth. Because the tensile strength of the filament must sustain the load resulting from the shear stress at the filament surface at a given filament radius the length of the fiber cannot exceed a certain value because otherwise the filament would break. When we consider a filament of length L and radius R the upper limit of its length L_{max} is given by:

$$L_{max} = \frac{\sigma' R^2 (1 - \ln K)}{2\eta V} \qquad [23]$$

where σ' is the tensile strength of the filament. In order to prevent the fiber from breaking (or, in other words, to obtain a stable growth process) the radial growth of the very thin primary filament just after formation must exceed a certain value, given by

$$\frac{dR}{dt} \geq \frac{2\eta V}{\sigma' R \{1 - 2 \ln K\}} \frac{dL}{dt}. \qquad [24]$$

5. Axial and radial growth

With the knowledge of driving force and shear stresses at the fiber wall, it is now possible to calculate the growth of the fiber. We suppose that the primary growth consists of two parts, an axial growth at the tip and an initially rapid radial growth that slows down at increasing fiber diameters and becomes approximately zero when the fiber reaches the final diameter of primary growth (40 μm in the experiments of *McHugh* et al. (10)). Eq. [8] gives a relation for the driving force for the growth of a fiber in a flow field, and the fiber will actually grow as long as this driving force exceeds a critical value. If we assume that this critical value is small compared with the individual terms of eq. [8] (this is generally the case), we can define a critical value of the entropy drop which the actual flow induced entropy drop has to exceed in order to make the fiber grow:

$$\Delta S_{crit} = \Delta H \left(\frac{1}{T_d} - \frac{1}{T} \right) \qquad [25]$$

where T_d is the dissolution temperature. This critical value is of course only meaningful if the actual temperature of the solution exceeds the dissolution temperature since for $T_d > T$ the polymeric material will crystallize even in the absence of a flowfield. The enthalpy per unit volume ($\Delta H \cdot c$) is within reasonable limits equal to the heat of fusion ($2.8 \cdot 10^8$ J/m^3) (17). Under the assumption of a contravariant Maxwell model as a constitutive equation, the entropy drop due to flow can be obtained from a combination of eqs. [10] and [13]:

$$\Delta S_{flow} = \frac{\Delta \eta \dot{\Gamma}_{rz}^2}{c T}, \qquad [26]$$

and a combination of this result with eq. [25] leads to the conclusion that the fiber will grow until the shear rate at the wall reaches a critical value given by:

$$\dot{\Gamma}_{rz} = \left[\frac{\Delta H c}{\Delta \eta} \theta \right]^{1/2} \qquad [27]$$

where θ is the relative temperature which can be expressed in terms of the absolute temperatures

$$\theta = \frac{T - T_d}{T_d}. \qquad [28]$$

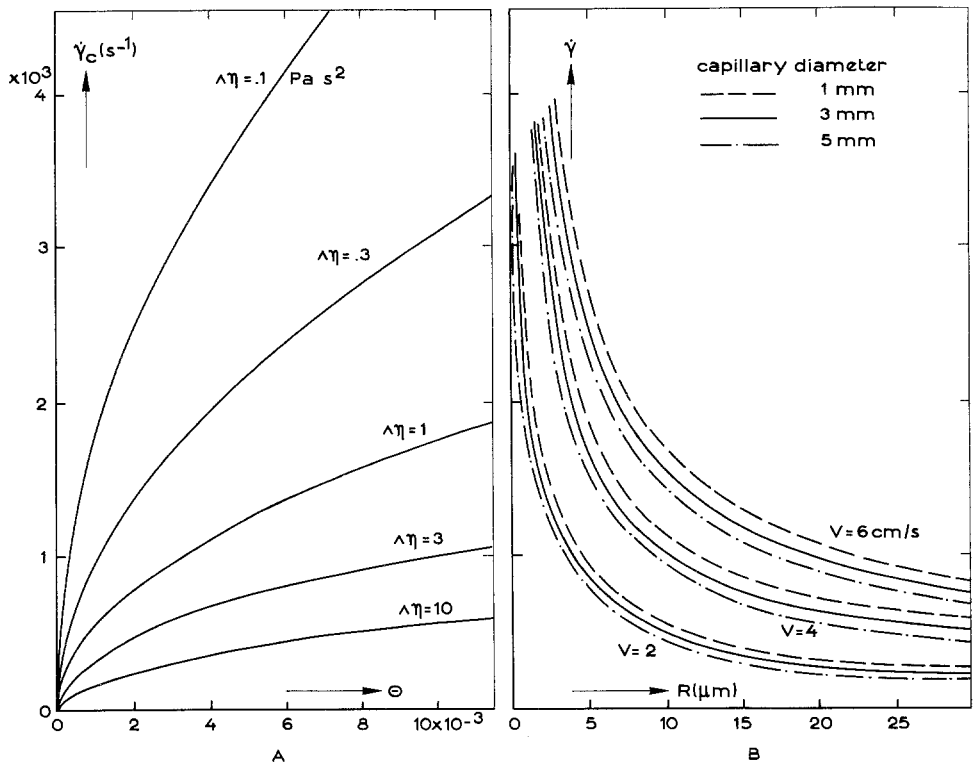

Fig. 5. a) Critical shear rate at the fiber wall as a function of relative temperature and rheological properties of the solution. – b) Shear rate at the fiber wall as a function of the fiber-radius, the relative velocity and the capillary diameter. (The vertical axes have the same scale.)

The final diameter of the fiber will be reached when the radius is such that the shear rate of the wall (as expressed by eq. [15]) coincides with the critical shear rate:

$$R_c(1 - \ln K_c) = V\left[\frac{\Lambda\eta}{\Delta H c\theta}\right]^{1/2} \qquad [29]$$

which is an implicit function for the final radius. Figure 5 gives the results of these calculations in a quantitative way. The left graph shows the dependency of the critical shear rate at the wall as a function of the temperature with the rheology of the solution as parameter, the right graph shows the flow induced shear rate (at the same scale as the left graph) as a function of the fiber radius with the relative velocity between the moving fiber and the undisturbed center velocity in an empty pipe as well as the capillary diameter as parameters.

5.1. The influence of the distribution functions on the growth process

In the previous part we have given an engineering approach to describe the fiber growth process. However, it has to be realized that the entropy change due to flow is an average value, there exists a distribution in the stretching and orientation of the molecules. Even if this entropy change due to flow is slightly smaller than the critical value, the molecules that have a larger stretching than the average can crystallize and the fiber will grow, although very slowly. Analogously, when the average entropy drop is slightly higher than the critical value, not all molecules are in the right shape to contribute to the growth. At this point it is interesting to compare the efficiency for the crystallization process of elongational flow and shear flow. In a shear flow the molecules have a tendency to tumble. Once a molecule is aligned with the flow a small disturbance in its orientation can cause the molecule to tumble around. On the other hand, an elongational flow is stabilizing. Once a molecule is aligned with the flow, every disturbance in this alignment will immediately be damped out. Because of this difference in rotational freedom, the width of the orientation and stretching distribution of the molecules in an elongational flow will be smaller than that in a

shear flow. This implies that, when the average free energy of the molecules in the flow is higher than the critical value, an elongational flow is more effective than a shear flow, even if the trace of the stress tensor is the same for both flow fields, as shown in figure 6a. If, on the other hand, the average free energy is slightly lower than the critical value, the shear flow still can give rise to some growth while the elongational flow is ineffective (fig. 6b).

5.2. *The crystal growth equations in connection with the distribution functions of the molecules in the fluid*

The difference in distribution functions between shear flow and elongational flow has also its consequences for the growth phenomena of the fiber.

At it has been pointed out by *Lauritzen* and *Hoffman* (17) polymer molecules generally crystallize in a folded chain conformation, and the growth front proceeds perpendicular to the chain direction. Assuming a surface nucleation mechanism, they calculated the growth rate and the length of the chain folds as a function of the driving force, $\Delta\mu$. The growth rate G is given by:

$$G = G^* \exp\{-\alpha b \sigma \sigma_e / \Delta\mu R^* T\} \qquad [30]$$

where G^* includes the diffusion process to the crystal and some specific crystal parameters, α is 2 or 4 depending on the nucleation model, b is the surface layer thickness, σ is the lateral surface free energy, and σ_e is the fold surface free energy.

From this formula it can be seen that generally chain folding is preferred over extended chain crystallization because of kinetic reasons, since it has the lowest fold surface free energy σ_e and therefore the highest growth rate.

At a certain driving force the average fold length has a value a little bit higher than $l = 2\sigma_e/(\Delta\mu)$, the length of the critical nucleus.

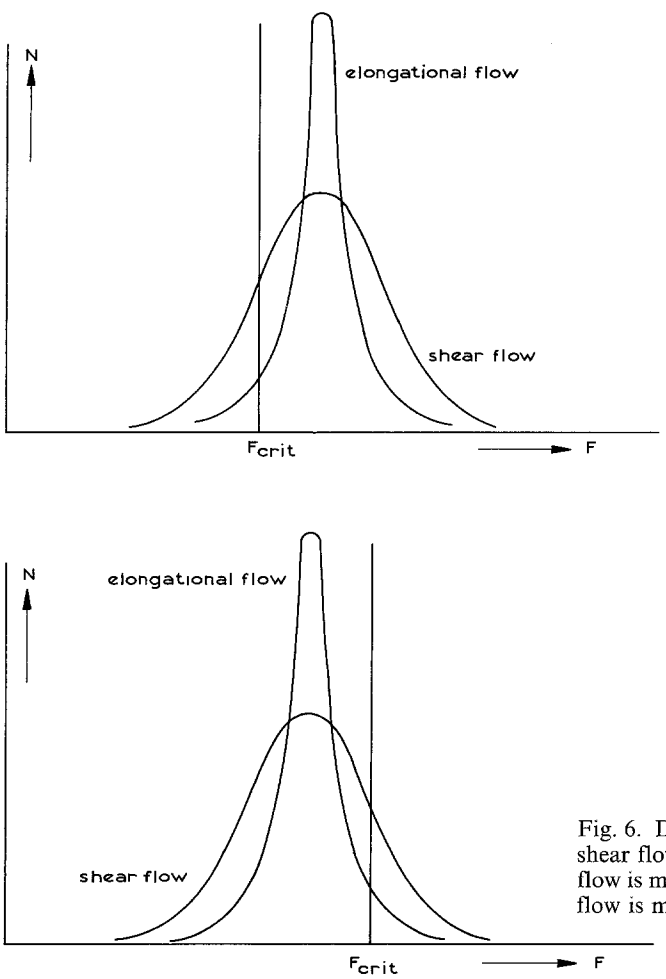

Fig. 6. Distribution function of the free energy for shear flow and elongational flow. a) The elongational flow is more effective than the shear flow. b) The shear flow is more effective than the elongational flow

When $\Delta\mu$ is not too high, the fold length can be approximated by this value.

These formulas for the growth rate and the fold length are derived for stagnant solutions or melts. It is assumed that they do not apply to the inner part of the fiber that is favored by extensional flow. *Elyashevich* et al. (28) have developed a thermodynamical analysis about the decrease of conformational entropy owing to the drawing of a molecule into a crystal. They showed that, below a certain extension of the molecule, the crystallization with the formation of folded chain crystals is thermodynamically preferable, and above that value extended chain crystals are formed. Although this theory is not coupled to a certain flow field, it is assumed that extensional flow may provide the right conditions.

We will now consider the radial growth of the fiber in connection with the crystal growth equations. Taking the distribution function for a shear flow into account (fig. 6), it is easy to see that the driving force varies from a certain value that is determined by the concentration of the solution (see eq. [9]) to that of a completely extended chain. This means that the growth rate and the fold length also vary.

If the driving force is zero because of the concentration, the average value of $\Delta\mu = \langle T\Delta S\rangle_{\text{flow}}$. That means for this case that from the point of view of crystal growth we can expect every fold length between the length of the critical nucleus and the length of an extended molecule, with a maximum percentage having a length a little bit larger than $l = 2\sigma_e/\langle T\Delta S\rangle_{\text{flow}}$.

When we raise the temperature a few degrees without changing the concentration of the solution, the value of $\langle T\Delta S\rangle_{\text{flow}}$ does not change much, but the difference in chemical potential between molecules in the solution far from the fiber and in the crystal $(F_V - F_K)$ becomes more negative (see fig. 1). Although the free energy content goes up by an amount $|T\Delta S|_{\text{flow}}$ near the surface, this still gives a lower value of the driving force. This means that the average fold length becomes larger. This explains why the mechanical properties of a fiber are better when it is grown at a higher crystallization temperature (29).

6. Conclusions

In spite of existing uncertainties that make it necessary to adopt some rough order-of-magnitude estimations, it was possible to obtain a quantitative prediction for the growth of fibers from solution.

The driving force for this process is partly caused by the difference in chemical potential between the solute molecules and the molecules in the fiber because of the concentration of the solution (at temperatures above the dissolution temperature this difference is negative), and partly by the decrease of the communal entropy (χ) and internal entropy (S^f) of a solute molecule because of the flow field. Assuming a Maxwell fluid, which means that the molecules are considered as elastic dumbbells, the decrease of entropy can be calculated under the restriction that the influence of entanglements can be neglected (21). This means, of course, low concentrations of the solutions. It appeared that under these restrictive assumptions the decrease in entropy because of a certain flow field can be added to the classical no-flow result, where the driving force is linearly proportional to the supersaturation.

In this paper the growth of a fiber in Poiseuille flow is considered. The shear stress at the wall of a filament can reduce the entropy of the polymer molecules to such an extent that radial growth occurs even at high crystallization temperatures, although this growth goes rapidly to zero when the fiber reaches its final diameter. This final diameter, reached when the entropy drop at the fiber wall equals a critical value, is among others a function of the rheology of the solution and, therefore, through viscosity and relaxation time coupled with the concentration and the molecular weight of the polymer used. Since the drop in conformational entropy is quadraticly proportional to the relative velocity between the fiber wall and the undisturbed fluid flow, an external velocity field apart from that which originates from the fiber drawing seems extremely helpful.

The axial growth of the primary filament originates from the elongational flow at the fiber tip. Although the total elongation of the molecules in this field is expected to be very large this is not of much use before the fiber starts growing, since the elongated molecules will not reach the fiber tip. Only molecules that are (partially) stretched by the shear flow at the seed walls and attached to the seed just before leaving the tip can contribute to the initiation of the axial growth. Once the fiber starts growing

it grows very rapidly since the elongated molecules can reach the tip very easily.

Also the strength of the fiber can be important. Although it has no significance for fibers near their final diameter, it is an important restriction for the very thin primary fibril that may form at the tip. Considering for instance such a fibril of 100 Å diameter for polyethylene ($\sigma' < 1.27 \cdot 10^{10}$ Pa) in a 1 Pa s solution flowing with a relative velocity of 4 cm/s it appears that this filament must have a length of less than 3.6 mm. This implies that if one tries to improve the axial growth too much without increasing the radial growth the filament will break and the whole process might become unstable. Knowledge of the actual extension flow at the tip is still lacking and it is clear that more research in this area has to be done.

From crystal growth point of view, it can be seen that because of the need for larger extension of the molecules in order to crystallize at higher temperatures, fibers that are grown at higher temperatures must have better mechanical strength than fibers grown at a lower temperature. This is shown experimentally by *Zwijnenburg* and *Pennings* (29).

Acknowledgments

The authors wish to thank Professors *A. B. Metzner, R. L. McCullough* and *A. J. McHugh* for the stimulating discussion. Special acknowledgment is due to Professor *G. Astarita* for help and the numerous discussions.

Part of this work is supported by the Netherlands Organization for Advancement of Pure Research (ZWO).

Summary

An engineering model of fiber growth from a flowing solution is presented. Attention is focussed on three main issues: the fluid mechanics, the molecular structure of the fluid, coupled with the thermodynamics, and the crystal growth itself. Although because of existing uncertainties order of magnitude analyses had to be adopted it was possible to obtain quantitative predictions about the growth process.

Zusammenfassung

Es wird ein einfaches Modell des Faserwachstums aus einer strömenden Lösung vorgestellt. Dabei werden vor allem drei wesentliche Aspekte betrachtet: die Strömungsmechanik, die molekulare Struktur und Thermodynamik der Flüssigkeit, sowie das Kristallwachstum selbst. Obgleich wegen der noch bestehenden Unsicherheiten nur größenordnungsmäßige Abschätzungen in Ansatz gebracht werden konnten, war es dennoch möglich, quantitative Aussagen über den Wachstumsvorgang zu erhalten.

References

1) Symposium on Stress-Induced Crystallization, Polym. Eng. Sci. **16** (1976).

2) *Pennings, A. J.*, Symposium on Macromolecular Chemistry, preprint 216 (Prague 1965); J. Polym. Sci. Part. C, **16**, 1799 (1967).

3) *Pennings, A. J., A. M. Kiel*, Kolloid. Z. u. Z. Polymere **205**, 160 (1965).

4) *Pennings, A. J.*, Crystal Growth, Proc. Int. Conf. on Crystal Growth, pp. 389–393, Boston (Oxford 1966).

5) *McHugh, A. J., E. H. Forrest*, J. Macromol. Sci.-Phys. **B 11**, 219 (1975).

6) *McHugh, A. J.*, J. of Appl. Pol. Sci. **19**, 125 (1975).

7) *McHugh, A. J., C. Silebi*, Pol. Eng. Sci. **16**, 158 (1976).

8) *Zwijnenburg, A., A. J. Pennings*, Coll. Polym. Sci. **253**, 452 (1975).

9) *Zwijnenburg, A., A. J. Pennings*, Coll. Polym. Sci. **254**, 868 (1976).

10) *McHugh, A. J., P. Vaughn, E. Ejike*, Pol. Eng. Sci. **18**, 443 (1978).

11) *Hill, J. L.*, Statistical Mechanics, McGraw-Hill (New York 1956).

12) *van der Eerden, J. P., P. Bennema, T. A. Cherapanova*, Progress in Crystal Growth and Assessment, no. 3, Pergamon Press (Oxford 1977).

13) *Astarita, G.*, Pol. Eng. Sci. **14**, 730 (1974).

14) *Astarita, G., G. C. Sarti*, J. Non-Newtonian Fluid Mech. **1**, 39 (1976).

15) *Glasstone, S., K. J. Laidler, H. Eyring*, The Theory of Rate Processes (New York 1941).

16) *Janssen-van Rosmalen, R., P. Bennema, J. Garside*, J. of Crystal Growth **29**, 342 (1975).

17) *Hoffman, J. D., G. T. Davis, J. I. Lauritzer*, J., Treatise Solid State Chem. **3**, 497–614 (1976).

18) *Astarita, G., G. Marucci*, Principles of Non-Newtonian Fluid Mechanics, McGraw-Hill (Maidenhead 1974).

19) *Peterlin, A.*, Pol. Eng. Sci. **16**, 126 (1976).

20) *Astarita, G., G. C. Sarti*, J. Non-Newtonian Fluid Mech. **3**, 77 (1977).

21) *Marrucci, G.*, Trans. Soc. Rheol. **16**, 321 (1972).

22) *Mackley, M. R.*, Colloid & Polym. Sci. **253**, 373 (1975).

23) *Mackley, M. R., A. Keller*, Phil. Trans. Roy. Soc. (Lond.) **278** (1276), 29 (1975).

24) *Mackley, M. R., F. C. Frank, A. Keller*, J. of Mat. Sci. **10**, 1501 (1975).

25) *Denn, M. M.*, The Mechanics of Viscoelastic Fluids, AMD-vol. 22, ASME (New York 1977).

26) *Schlichting, H.*, Boundary layer theory, p. 222, McGraw-Hill (New York 1968).

27) *McHugh, A. J.*, private communications.

28) *Elyashevich, G. K., V. G. Baranov, S. Ya. Frenkel*, J. Macromol. Sci. Phys. **B 13** (2), 255 (1977).

29) *Zwijnenburg, A., A. J. Pennings*, Polym. Letters Ed. **14**, 339 (1976).

Authors' address:
Dr. ir. *L P. B. M. Janssen*
Laboratorium voor Fysische Technologie
Delft University of Technology
Prins Bernhardlaan 6
Delft (The Netherlands)